NASA TN D-140

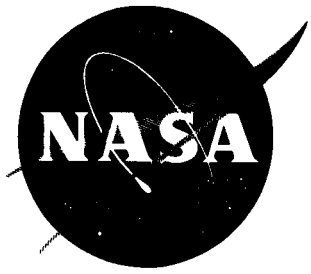

TECHNICAL NOTE
D-140

DISSOCIATIVE RELAXATION OF OXYGEN OVER AN ADIABATIC FLAT PLATE AT HYPERSONIC MACH NUMBERS

By Paul M. Chung and Aemer D. Anderson

Ames Research Center
Moffett Field, Calif.

NATIONAL AERONAUTICS AND SPACE ADMINISTRATION

WASHINGTON

April 1960

NATIONAL AERONAUTICS AND SPACE ADMINISTRATION

TECHNICAL NOTE D-140

DISSOCIATIVE RELAXATION OF OXYGEN OVER AN ADIABATIC FLAT PLATE AT HYPERSONIC MACH NUMBERS

By Paul M. Chung and Aemer D. Anderson

SUMMARY

The integral method was used to study the dissociative relaxation phenomena of pure oxygen over an adiabatic flat plate at hypersonic Mach numbers.

By means of the integral method, a solution was obtained, with relative ease, to a problem involving finite rate dissociation and recombination in a hypersonic laminar boundary layer.

It was found that dissociative equilibrium is never approximated over an adiabatic flat plate of reasonable length when the conditions of the free stream are those of the atmosphere at the altitude range from 50,000 to 200,000 feet and Mach numbers from 10 to 20.

It is predicted on the basis of the present analysis that heat transfer to a highly cooled flat plate may be quite closely approximated by the values of heat transfer across a chemically inert boundary layer with the same total energy per unit mass of the free-stream gas, at least for Mach numbers below 20 at the altitudes considered here.

INTRODUCTION

In hypersonic flight, chemical reactions begin to play an important role in aerodynamic heat transfer. Dissociation occurs across the strong bow shock waves formed by a blunt body, and the dissociated radicals predominantly recombine within the gas or on the surface as they flow along the body.

The shock wave formed by a slender body, on the other hand, is quite weak and the Mach number downstream from the shock is of the order of that in the free stream. In this case, the gas-phase reaction is predominantly that of dissociation in the boundary layer because of the high viscous dissipation.

These problems have been analyzed by several people and a rather complete resumé of the work appears in references 1 and 2. A review of the existing literature on the problem, however, reveals that most of

the theoretical work on the subject has been limited to a few specific cases, where the gas-phase chemical reactions have usually been assumed to occur at an infinitely fast rate when they occur at all. This basic assumption implies that the chemical reactions are completely controlled by the transport characteristics of the boundary layer. The problem then can be solved using, with little modification, the conventional boundary-layer analysis, and affine solutions to the problem can usually be obtained.

Most studies which included surface reactions have considered the gas-phase reaction to be chemically frozen. The chemical reactions in the gas phase, however, usually occur at finite rates. The consideration of finite reaction rates involves chemical reaction kinetics and incorporating them into the boundary-layer analysis usually results in a breakdown of the affine characteristics of the boundary-layer equations.

Only at the stagnation region of blunt bodies can the conventional affine transformation be used to solve the exact boundary-layer equations including the effect of finite chemical reaction rates. Some of these solutions were obtained in references 3 and 4. Aside from the stagnation region in which the velocity of the gas at the edge of the boundary layer is a linear function of the distance along the surface, the usual method of transformation fails to transform the partial differential equations of the boundary layer into a set of ordinary differential equations when finite chemical reaction rates are included.

There seem to be two methods existing today which may, in general, be used to solve the problems of hypersonic laminar heat transfer with finite rate dissociation and recombination. The first is a modified application of the von Karmán integral method. This method was used successfully in reference 5 to solve a problem of ignition and combustion in a laminar mixing zone of two parallel streams of equal velocity. The second involves integrating the boundary-layer equations directly with respect to the independent variables of the partial differential equations by a rather complicated iteration technique. This method was described in reference 6 and it was applied to some problems of ignition in a laminar boundary layer.

The present work is primarily concerned with investigating the use of the first method in solving problems involving finite rate chemical reactions of air in hypersonic laminar boundary layers. The first method is chosen here because it seems to be less complicated and more flexible in applications.

The simple physical model used for the primary purpose stated is the nonequilibrium dissociation of pure oxygen over an adiabatic and noncatalytic flat plate. The second purpose of the present work is to study, for the particular physical model considered, the dissociative relaxation phenomenon of oxygen in hypersonic laminar boundary layers.

SYMBOLS

C	$\frac{\rho\mu}{\rho_\infty\mu_\infty}$
c_p	specific heat, cal/gram ^oK
$\bar{c}_p$	specific heat of the mixture, cal/gram ^oK
D	binary diffusion coefficient, cm^2/sec
f	$\frac{u}{u_\infty}$
F_1	integral defined by equation (12)
F_2	integral defined by equation (13)
F_3	integral defined by equation (14)
h	total enthalpy defined by equation (19), cal/gram
h^o	heat of formation at absolute zero, cal/gram
Δh^o	heat of dissociation of O_2, cal/gram
k	thermal conductivity, cal/sec cm ^oK
k_d	specific dissociation rate coefficient, $cm^3/mole\ sec$
k_r	specific recombination rate coefficient, $cm^6/mole^2\ sec$
K_p	equilibrium constant based on partial pressures, atm
L	reference length, cm
Le	Lewis number, $\frac{Pr}{Sc}$
m	mass fraction
M	molecular weight, gram/mole
M_∞	Mach number of the free stream
p	pressure, atm
Pr	Prandtl number, $\frac{\mu\bar{c}_p}{k}$

R_u universal gas constant, cm^3 atm/mole ^oK

r temperature recovery factor

Re Reynolds number, $\frac{\rho_\infty u_\infty L}{\mu_\infty}$

Sc Schmidt number, $\frac{\mu}{\rho D}$

T temperature, ^oK

u x-component of velocity, cm/sec

v y-component of velocity, cm/sec

w_1 net production rate of atoms per unit volume, gram/sec cm^3

x distance and direction parallel to the plate, cm unless otherwise specified

y distance and direction normal to the plate, cm

Γ specific reaction rate defined by equation (34)

γ ratio of the specific heats of the free-stream gas

δ boundary-layer thickness, cm

η dimensionless ordinate defined by equation (11)

θ $\frac{T}{T_\infty}$

λ dimensionless variable defined by equation (9)

μ absolute viscosity, dyne sec/cm^2

ξ $\frac{x}{L}$

ρ density, gram/cm^3

Subscripts

i ith species

1 atoms

2 molecules

o at the wall

∞ free-stream condition

Superscript

' total differentiation with respect to ξ

ANALYSIS

Conservation Equations

A flat plate with an infinitely sharp leading edge is considered to be located in a uniform stream of molecular oxygen at hypersonic Mach numbers as shown in figure 1.

The following conservation equations are obtained for a steady laminar boundary layer over the plate where the streamwise pressure gradient due to the boundary-layer displacement thickness is ignored. The effects of radiation and thermal diffusion are neglected.

$$\frac{\partial \rho u}{\partial x} + \frac{\partial \rho v}{\partial y} = 0 \qquad \text{continuity} \qquad (1)$$

$$\rho u \frac{\partial u}{\partial x} + \rho v \frac{\partial u}{\partial y} = \frac{\partial}{\partial y}\left(\mu \frac{\partial u}{\partial y}\right) \qquad \text{momentum} \qquad (2)$$

$$\rho u \frac{\partial h}{\partial x} + \rho v \frac{\partial h}{\partial y} = \frac{\partial}{\partial y}\left\{\frac{k}{\bar{c}_p}\left[\frac{\partial h}{\partial y} - (1-Pr)\frac{\partial (u^2/2)}{\partial y} - (1-Le)\sum_{i=1}^{2} h_i \frac{\partial m_i}{\partial y}\right]\right\} \qquad \text{total energy} \qquad (3)$$

$$\rho u \frac{\partial m_1}{\partial x} + \rho v \frac{\partial m_1}{\partial y} = \frac{\partial}{\partial y}\left(\rho D \frac{\partial m_1}{\partial y}\right) + w_1 \qquad \text{diffusion} \qquad (4)$$

The boundary conditions are:

at $y = 0$

$$u = 0$$

$$v = 0$$

$$\frac{\partial h}{\partial y} = 0$$

$$\frac{\partial m_1}{\partial y} = 0$$

at $y = \infty$

$$u = u_\infty$$

$$h = h_\infty$$

$$m_1 = 0$$

The equation of state for the mixture is

$$p = (1 + m_1)\ \rho \frac{R_u}{M_2} T \tag{5}$$

For the purpose of simplification, both the Prandtl number and the Lewis number are assumed to be equal to 1. This assumption does not alter the basic results. The energy equation (3) then becomes

$$\rho u \frac{\partial h}{\partial x} + \rho v \frac{\partial h}{\partial y} = \frac{\partial}{\partial y}\left(\mu \frac{\partial h}{\partial y}\right) \tag{6}$$

The exact solution which satisfies equation (6) and the boundary conditions is $h = h_\infty$ for all x and y. The remaining conservation equations (1), (2), and (4) are solved here by first integrating them across the boundary layer.

A comparatively simple application of the integral method to compressible laminar boundary layers is given in reference 7 and is used here. The essential simplification is accomplished by integrating all the conservation equations in the y direction from the wall to the edge of the momentum boundary layer, and by assuming $\rho\mu/\rho_\infty\mu_\infty = C$ to be constant. According to reference 2, the effect of this assumption is small when the constant C is properly chosen. The use of a single boundary-layer thickness here does not impose any undue restrictions on the problem because

(1) Prandtl and Lewis numbers are assumed to be equal to unity.

(2) The polynomial expression which is used here for the atom concentration profile, thus also the temperature profile, is permitted to contain an additional coefficient not determined in advance by the boundary conditions in accordance with the method described in reference 7.

The continuity equation is incorporated into the momentum and the diffusion equations, and the integration of these equations across the boundary layer yields the following integro-differential equations

$$\left(\frac{F_1}{2}\right)\lambda' + F_1'\lambda = \left[\frac{\partial(u/u_\infty)}{\partial\eta}\right]_0 \tag{7}$$

$$\left(\frac{F_2}{2}\right)\lambda' + F_2'\lambda = F_3 \tag{8}$$

where

$$\lambda = \left(\frac{\hat{\delta}}{L}\right)^2 \frac{Re}{C} \tag{9}$$

$$\hat{\delta} = \int_0^\delta \frac{\rho}{\rho_\infty}\, dy \tag{10}$$

$$\eta = \frac{\int_0^y \frac{\rho}{\rho_\infty}\, dy}{\int_0^\delta \frac{\rho}{\rho_\infty}\, dy} \tag{11}$$

$$F_1 = \int_0^1 \frac{u}{u_\infty}\left(1 - \frac{u}{u_\infty}\right) d\eta \tag{12}$$

$$F_2 = \int_0^1 \left(\frac{u}{u_\infty}\right) m_1 d\eta \tag{13}$$

$$F_3 = \frac{\lambda L}{u_\infty} \int_0^1 \frac{w_1}{\rho}\, d\eta \tag{14}$$

The main addition to the conventional integro-differential equations is F_3, given by equation (14). The behavior of equation (8) will largely depend on the behavior of the integral F_3.

The integral method was used in reference 8 in the study of the same problem of dissociation of oxygen over an adiabatic flat plate. The reaction rate term w_1, however, which appears in the integral F_3 was a priori assumed to be a known function of η in the reference. The diffusion equation was, therefore, linearized and this afforded an immediate integration of equation (14). This rather arbitrary approximation does not yield any quantitative information for finite values of x, and the work was limited to estimating the length at which equilibrium conditions were approached.

The reaction rate w_1 is obtained from chemical kinetics and this phase will be considered in the next section.

Homogeneous Chemical Reactions

The kinetics of oxygen molecule-atom reaction have been considered in several places in the literature. It is known that dissociation is a second-order reaction whereas recombination is a third-order reaction (see ref. 9 for the definition of order of reaction). Thus, the reversible reaction can be expressed as:

$$A_1 + A_1 + X \underset{k_d}{\overset{k_r}{\rightleftarrows}} A_2 + X \tag{15}$$

where A_1 and A_2 are the mole concentrations of atoms and molecules, respectively, and X presents the mole concentration of a third particle which must be present to activate the reaction. For the present case of an oxygen atom and molecule mixture, X is the total number of moles per unit volume of the mixture.

The law of mass action (see ref. 9) yields the following net production rate of atoms per unit volume of the mixture for the reaction represented by equation (15).

$$w_1 = -2XM_1k_r\left(A_1^2 - \frac{k_d}{k_r}A_2\right) \tag{16}$$

The form of the equation can be varied to suit the form of the conservation equations. The particular transformation used in reference 10 is followed here.

The ratio k_d/k_r can be evaluated at the equilibrium condition, and is defined as the equilibrium constant based on mole concentration. It is related to the equilibrium constant based on partial pressures by

$$k_d/k_r = K_p\frac{X}{p}$$

In reference 11 K_p is given as exp (15.8 - (60,000/T)). Details of the calculation of K_p can be found in reference 12. When the mole concentrations are written in terms of m_1 and the equation of state (5) is introduced, equation (16) becomes

$$\frac{w_1}{\rho} = -(2k_r)2\left(\frac{p}{R_u}\right)^2 \frac{1}{T^2}\left[\frac{m_1^2}{1+m_1} - \frac{1}{4p} K_p(1-m_1)\right] \tag{17}$$

Although much has been done elsewhere both theoretically and experimentally to determine the value of k_r as a function of temperature, it is still not too well known.

Reference 13 by means of a statistical analysis showed that the recombination coefficient should increase with temperature at lower temperatures but should decrease with temperature at the higher temperatures encountered in this study. According to the Wigner theory, as presented in reference 14, k_r is proportional to $T^{-1/2}$, a lesser decrease with temperature than was indicated by the statistical analysis. It is felt that the prediction of the Wigner theory is an upper limit on k_r in the temperature range considered here.

Recent experimental measurements of k_r are reported in references 15 and 16. Both studies showed k_r to vary as $1/T^2$. These values are less than those of the Wigner theory and the functional variation with temperature is in essential agreement with the statistical analysis. The values obtained in reference 15 were about twice those obtained in reference 16. Although the choice between the two is somewhat arbitrary, the expression used here is based upon the data of reference 15. It is

$$2k_r = \frac{1.98\times10^{22}}{T^2}\left(\frac{cm^6}{mole^2\ sec}\right)$$

The final expression of the reaction term becomes

$$\frac{w_1}{\rho} = -(1.98\times10^{22})2\left(\frac{p}{R_u}\right)^2 \frac{1}{T^4}\left[\frac{m_1^2}{1+m_1} - \frac{1}{4p}\exp\left(15.8 - \frac{60,000}{T}\right)(1-m_1)\right] \tag{18}$$

SOLUTION OF EQUATIONS FOR ADIABATIC TEMPERATURES

The previously derived equations are used here to solve for the adiabatic temperatures.

The total enthalpy h is given by:

$$h = \sum_i h_i m_i + \frac{u^2}{2} \tag{19}$$

where

$$h_i = \int_o^T c_{p_i} dT + h_i^o \tag{20}$$

Consider c_{p_i} for oxygen atoms and molecules. Figure 4 of reference 17 shows that the specific heat of atomic oxygen is a constant and that the specific heat of molecular oxygen varies appreciably at lower temperatures but becomes practically invariant with temperature above about 2000° K. Therefore, c_{p_i} is assumed to be constant. The expression for total enthalpy now becomes:

$$h = [m_1(c_{p_1}-c_{p_2}) + c_{p_2}]T + m_1\Delta h^o + u^2/2 \tag{21}$$

Now

$$m_1\left(\frac{c_{p_1}-c_{p_2}}{c_{p_2}}\right) << 1$$

Therefore

$$h \approx c_{p_2}T + m_1\Delta h^o + u^2/2 \tag{22}$$

It was shown in the section "Conservation Equations" that the solution of the energy equation for the present case is that h is constant throughout the flow field and is equal to the total energy in the free stream.

Equation (22) immediately yields the temperatures as a function of the atom mass fraction and the reduced velocity,

$$\frac{T}{T_\infty} = \theta = 1 + \left(\frac{\gamma-1}{2}\right) M_\infty^2(1-f^2) - \frac{\Delta h^o}{c_{p_2}T_\infty} m_1 \tag{23}$$

The first step in solving the integro-differential equations (7) and (8) is to assume appropriate profiles for the velocity and the mass fraction. A sixth degree polynomial is assumed for the velocity profile and one of fifth degree for the atom mass fraction profile as:

$$\frac{u}{u_\infty} \equiv f(\eta) = \sum_{n=0}^{6} a_n \eta^n \tag{24}$$

$$m_1(\xi,\eta) = \sum_{n=0}^{5} b_n(\xi)\eta^n \tag{25}$$

The boundary conditions for equations (24) and (25) which are obtained with the aid of equations (2), (4), and (18) are:

at $\eta = 0$

$$\left.\begin{aligned} f &= 0 \\ \frac{\partial^2 f}{\partial \eta^2} &= 0 \\ \frac{\partial^3 f}{\partial \eta^3} &= 0 \\ \frac{\partial m_1}{\partial \eta} &= 0 \\ \frac{\partial^2 m_1}{\partial \eta^2} &= -\frac{\lambda L}{u_\infty}\frac{w_{1,o}}{\rho_o} \end{aligned}\right\} \tag{26}$$

at $\eta = 1$

$$\left.\begin{aligned} f &= 1 \\ \frac{\partial f}{\partial \eta} &= 0 \\ \frac{\partial^2 f}{\partial \eta^2} &= 0 \\ \frac{\partial^3 f}{\partial \eta^3} &= 0 \\ m_1 &= 0 \\ \frac{\partial m_1}{\partial \eta} &= 0 \\ \frac{\partial^2 m_1}{\partial \eta^2} &= 0 \end{aligned}\right\} \tag{27}$$

The momentum equation (7) with the sixth degree profile given by equation (24) was solved in reference 7 with the results:

$$f = 2\eta - 5\eta^4 + 6\eta^5 - 2\eta^6 \tag{28}$$

and

$$\lambda = \frac{36,036}{985}\,\xi \tag{29}$$

Application of the boundary conditions for m_1 given in equations (26) and (27) to the profile of (25) yields the following values for the coefficients $b_n(\xi)$.

$$\left.\begin{aligned} b_1 &= 0 \\ b_2 &= \frac{1}{2}\,\varphi\left(\frac{\lambda L}{u_\infty}\,,\ b_o\right) \\ b_3 &= -\frac{3}{2}\,\varphi\left(\frac{\lambda L}{u_\infty}\,,\ b_o\right) - 10b_o \\ b_4 &= \frac{3}{2}\,\varphi\left(\frac{\lambda L}{u_\infty}\,,\ b_o\right) + 15b_o \\ b_5 &= -\frac{1}{2}\,\varphi\left(\frac{\lambda L}{u_\infty}\,,\ b_o\right) - 6b_o \end{aligned}\right\} \tag{30}$$

where

$$\varphi\left(\frac{\lambda L}{u_\infty}\,,\ b_o\right) = \left(\frac{\lambda L}{u_\infty}\right) \frac{(1.98\times10^{22})2\left(\frac{p}{R_u}\right)^2}{\left[1 + \left(\frac{\gamma-1}{2}\right)M_\infty^2 - \frac{\Delta h^o}{c_{p_2}T_\infty}\,b_o\right]^4 T_\infty^4} \left\{ \frac{b_o^2}{1+b_o} - \frac{1}{4p}\exp\left[15.8 - \frac{60,000}{T_\infty\left(1 + \frac{\gamma-1}{2}\,M_\infty^2 - \frac{\Delta h^o}{c_{p_2}T_\infty}\,b_o\right)}\right](1-b_o)\right\} \tag{31}$$

Now the two integrals, F_2 and F_3, given by equations (13) and (14), respectively, become:

$$F_2 = \frac{5}{7}\,b_o + \frac{79}{252}\,b_2 + \frac{29}{120}\,b_3 + \frac{97}{495}\,b_4 + \frac{38}{231}\,b_5 \tag{32}$$

and

$$F_3 = -\Gamma \int_0^1 \frac{1}{[\theta(\xi,\eta)]^4} \left\{ \frac{m_1^2(\xi,\eta)}{1+m_1(\xi,\eta)} - \frac{1}{4p} \exp\left[15.8 - \frac{60{,}000}{T_\infty \theta(\xi,\eta)} \right] [1-m_1(\xi,\eta)] \right\} d\eta \tag{33}$$

where

$$\Gamma = (1.98\times10^{22})2 \left(\frac{p}{Ru}\right)^2 \frac{1}{T_\infty{}^4} \left(\frac{\lambda L}{u_\infty}\right) \tag{34}$$

In equation (33) F_3 represents the effect of the chemical reaction and the main problem remaining is to find its effect on the solution of the diffusion equation (8). Equation (33) can be considered to be made up of two separate functions. The first, Γ, represents the specific reaction rate and is solely dependent on the flight conditions of the vehicle. The higher the altitude and the speed of flight, the smaller is the specific rate Γ. The second, the integrand, represents the degree of departure of the fluid from the equilibrium state. Then for a relatively undissociated gas, the higher the altitude and the speed of flight the greater is the departure from the equilibrium state.

It is seen from the preceding discussion that the two effects in the reaction term, F_3, act in opposite directions with respect to flight conditions - at least near the leading edge of the body. This effect will be discussed further after some numerical examples are calculated.

It is noted here that the constant, C, appears only through the parameter λ in the entire analysis. This means that the solution of the problem is independent of the particular value of C assumed. It is only important that C remains constant throughout the analysis.

The integration of equation (8) must begin at the leading edge of the plate. It is essential to the success of the method that the function F_2 and its derivative be well behaved at $\xi = 0$. The atom concentration is zero everywhere for $\xi \leq 0$; F_2 is therefore zero for $\xi = 0$. The limiting value of the derivative of F_2 is obtained as follows. Equation (8) may be written:

$$F_2' = \frac{F_3 - (F_2/2)\lambda'}{\lambda' \xi} \tag{35}$$

where λ' is constant as is seen from equation (29). Evaluation of equation (35) shows that $\lim_{\xi \to 0} F_2' \to 0/0$. Application of L'Hospital's rule then yields:

$$\lim_{\xi \to 0} F_2' = \frac{\Gamma}{6p\lambda'} \int_0^1 \frac{1}{\theta(0,\eta)^4} \exp\left[15.8 - \frac{60{,}000}{T_\infty \theta(0,\eta)}\right] d\eta$$

where

$$\theta(0,\eta) = 1 + \left(\frac{\gamma-1}{2}\right) M_\infty^2 (1-f^2)$$

Therefore, F_2' is seen to be well behaved at the leading edge.

Finally, equation (8) is solved numerically by the use of an IBM 704 digital computer. The standard "Adams-Moulton Predictor-Corrector Variable Mode" method was readily applicable in the programing. Once programed, it took less than five minutes of machine time to complete a solution for x up to 15 feet.

In the numerical calculations, a value of 1.4 was used for the free stream γ. The parameter $\Delta h^\circ/c_{p_2}$ is 23,900° R, according to reference 4. Calculations were performed for values of pressure and free-stream temperature corresponding to atmospheric conditions at three altitudes. These values, which were obtained from reference 18, and the free-stream Mach numbers used are shown in the following table.

Altitude, ft	T_∞, °K	p_∞, atm	M_∞
50,000	218	0.1161	5, 10, 15
100,000	218	1.107×10^{-2}	10, 15, 20
200,000	348.9	3.727×10^{-4}	10, 15, 20

DISCUSSION

Typical profiles of atom mass fraction and temperature in the boundary layer at various positions along the flat plate are shown in figures 2 and 3, respectively.

It can be seen from figure 2 that the dissociation takes place primarily near the wall for the range of x considered here. This is to be expected because the viscous dissipation is greatest there and also the time available for the chemical reaction is large since the fluid is moving very slowly there.

According to equilibrium criteria for the oxygen atom-molecule reaction, practically no dissociation is expected below temperatures of about 2000° K at the pressure for which figures 2 and 3 are plotted. It is seen in figure 3 that temperature is below 2000° K in the outer half of the boundary layer. Dissociation, therefore, is confined to the

region adjacent to the wall within about 1/2 of the total boundary-layer thickness. Atoms diffuse into the outer portion of the boundary layer and there they recombine.

The profiles for the values of x considered here show a monotonic increase in atom concentration and a monotonic decrease in temperature, with x, throughout the boundary layer. The analysis of the preceding paragraphs shows that in the outer portion of the boundary layer the atom concentration must decrease and the temperature must increase as x is continuously increased beyond the range of x shown in figure 3. As x is increased, F_3 becomes large and begins to dominate equation (8), so that the fluid more nearly approaches equilibrium. The integral method used here can not be expected to satisfy the physical conditions at each point in the boundary layer. The profiles, however, at x of the order of 10^4 feet for instance, definitely show this correct trend. The boundary layer will of course become turbulent before such large values of x and the results of a laminar boundary-layer analysis are meaningless for such high values of x.

Figures 4(a) through 4(c) show the dissociative relaxation history of the gas at the wall for the various flight conditions. The percent of equilibrium dissociation at the wall is plotted against the actual distance measured along the plate from the leading edge. The equilibrium values of dissociation are shown for each case which enables one to determine the actual amount of dissociation.

It can readily be seen from the figures that, for the flight conditions considered here, equilibrium is not reached for reasonable values of x. At Mach number 15 and an altitude of 100,000 feet, for instance, $m_{1,o}$ would reach 99 percent of its equilibrium value at $x = 3{,}775$ feet. At 200,000 feet and the same Mach number it does not approach equilibrium this closely until x greater than 10,000 feet.

These arguments are based on the relaxation phenomena at the wall. Because of the low velocity near the wall, more time is available for the chemical reaction; therefore, the gas will approach the equilibrium state faster at the wall than at any other place in the boundary layer. For the cases considered here, it will take an unreasonably long distance of x for the entire boundary layer to relax completely.

The figures 4(a) through 4(c) can be analyzed more effectively in light of the reaction rate term F_3 given by equation (33). Near the leading edge, m_1 is rather small. The predominant portion of F_3 is then Γ and the second term of the integrand; therefore

$$\left| F_3 \right| \sim \left| \frac{p}{u_\infty} \exp \left[15.8 - \frac{60{,}000}{T_\infty \theta(\xi, \eta)} \right] \right| \tag{36}$$

The above equation shows that the reaction rate near the leading edge, for a given Mach number, is largely controlled by the pressure and it is directly proportional to it. Comparison of the three figures brings out this fact clearly - the lower the altitude, the higher the pressure and, therefore, the initial relaxation is faster.

The rate of relaxation with respect to length becomes faster near the leading edge as the Mach number is increased for all the cases shown in figures 4(a) through 4(c) except when the Mach number is increased from 15 to 20 at an altitude of 200,000 feet. It can be seen in equation (36) that, as the Mach number is increased for a given altitude, u_∞ tends to decrease the reaction rate while $T_\infty\theta$ tends to increase it. This fact was also discussed in the analysis section. The free-stream temperature at an altitude of 200,000 feet is 348.9° K whereas it is 218° K at the other two altitudes. Because of the increased free-stream temperature at 200,000 feet, the net effect of increasing the Mach number from 15 to 20 is a decrease in the relaxation rate at the leading edge.

The temperature recovery factor is plotted against Mach number in figures 5(a) and 5(b) for two different positions along the plate. The temperature recovery factor, r, for the present case is:

$$r(\xi) = 1 - \frac{\frac{\Delta h^\circ}{c_{p_2} T_\infty} b_0(\xi)}{\frac{(\gamma-1)}{2} M_\infty^2} \tag{37}$$

The equilibrium atom concentration is negligible for all x when M_∞ is small and the recovery factor is 1. It decreases as the Mach number is increased and atoms appear at the wall. According to equation (37), however, the recovery factor should start increasing at sufficiently high Mach numbers and should approach 1 as M_∞ is continually increased. The inversion point depends on the position along the flat plate as well as on the flight condition. It is seen in the figures that the lower the altitude, the higher the Mach number at which the inversion takes place.

Before concluding the present report, it may be interesting to investigate qualitatively and briefly the case of a highly cooled flat plate basing our predictions on the present analysis.

The temperature profile in a cooled compressible boundary layer of inert perfect gas with a Prandtl number of unity is given in reference 19 as:

$$\frac{T-T_0}{T_\infty} = \left(1 - \frac{T_0}{T_\infty}\right)\frac{u}{u_\infty} + \left(\frac{\gamma-1}{2}\right)M_\infty^2 \frac{u}{u_\infty}\left(1 - \frac{u}{u_\infty}\right) \tag{38}$$

If $T_o = 700^o$ K is assumed, the above equation indicates that the maximum temperature within the cooled boundary layer at $M_\infty = 20$ is about the same as the maximum recovery temperature which occurs at $M_\infty = 10$.

Now consider the following reaction rate law.

$$w_1 = -\Gamma \frac{1}{\theta^4} \left[\frac{m_1^2}{1+m_1} - \frac{1}{4p} \exp\left(15.8 - \frac{60{,}000}{T_\infty \theta}\right)(1-m_1) \right] \qquad (39)$$

As a first approximation, the terms in equation (39), excluding Γ, for gross rate of dissociation are of the same magnitude both for the cooled boundary layer at $M_\infty = 20$ and for the adiabatic one at $M_\infty = 10$. The specific reaction rate Γ is inversely proportional to M_∞ (see eq. (34)). The gross rate of dissociation, therefore, for the cooled boundary layer may be estimated to be about half of that for the adiabatic wall case. For the three altitudes, at $x = 10$ feet, the amount dissociated is estimated from figure 4 to be 5 percent of the total or less. Now, the maximum temperature occurs in the cooled boundary layer at a considerable distance from the wall. The atoms must pass through a highly cooled region before reaching the wall. The rate of recombination is very high in this region because of the low temperature. Of the 5 percent or less dissociated, it is very doubtful that any sizable amount of atoms could actually survive to reach the wall. The total enthalpy difference between the free stream and the wall is not varied by dissociation and recombination if all the atoms recombine before they reach the wall. Any difference in heat transfer from the inert case is due mainly to the variation in the values of the fluid properties, and this variation is usually small (see ref. 20). Therefore, the heat transfer to a wall at temperatures in the order of 700^o K through a hypersonic laminar boundary layer with dissociative relaxation may be estimated quite closely by calculating the heat transfer through an equivalent inert boundary layer using the total enthalpy difference. The present analysis, of course, is limited to temperatures and pressures corresponding to altitudes between 50,000 feet and 200,000 feet, and Mach numbers between 10 and 20.

On the other hand, the case of heat transfer through a laminar boundary layer behind a strong shock wave where the reaction is predominantly recombination is very important and the integral method should yield some interesting solutions.

CONCLUDING REMARKS

A theoretical study was made to investigate the use of the integral method in solving problems of the hypersonic laminar boundary layer with finite rate dissociation and recombination. The method was applied, in the present report, to a laminar boundary layer of pure oxygen over an adiabatic flat plate, and the phenomenon of dissociative relaxation caused by viscous dissipation was studied.

Solutions to the present problem were obtained with relative ease, and it seems that the integral method can be used for more complicated cases, in general, without any essential difficulties.

For most of the cases, the numerical solutions for the range of altitude of 50,000 to 200,000 feet and Mach numbers from 10 to 20 showed that the dissociative relaxation of oxygen due to the viscous dissipation is not sufficiently fast to justify an equilibrium approximation for reasonable lengths of the plate.

An estimation was made of the rate of chemical reaction within a highly cooled boundary layer and its effect on the heat transfer. This estimation was based on the present solutions for the adiabatic boundary layer. It showed that the effect of finite rate dissociation and recombination on heat transfer may be almost negligible for highly cooled boundary layers.

Ames Research Center
National Aeronautics and Space Administration
Moffett Field, Calif., Sept. 2, 1959

REFERENCES

1. Rosner, Daniel E.: Recent Advances in Convective Heat Transfer With Dissociation and Atom Recombination. Jet Propulsion, vol. 28, no. 7, July 1958, pp. 445-451.

2. Lees, L.: Convective Heat Transfer with Mass Addition and Chemical Reactions. Third AGARD Combustion and Propulsion Panel Colloquium. Palermo, Sicily, March 17-21, 1958. Pergamon Press, N.Y., pp. 451-498.

3. Fay, J. A., and Riddell, F. R.: Theory of Stagnation Point Heat Transfer in Dissociated Air. Jour. Aero. Sci., vol. 25, no. 2, Feb. 1958, pp. 73-85, 121.

4. Scala, S. M.: Hypersonic Heat Transfer to Surfaces Having Finite Catalytic Efficiency. G. E. Co. Aerophysics Research Memo. No. 4, Document 57SD646, June, 1957.

5. Marble, Frank E., and Adamson, Thomas C., Jr.: Ignition and Combustion in a Laminar Mixing Zone. Selected Combustion Problems, Fundamentals and Aeronautical Applications: Combustion Colloquium, Cambridge University, England, Dec. 7 to 11, 1953. Pergamon Press, N.Y., 1954. (Also by Butterworth Scientific Publications, London, vol. 1, pp. 111-131, and CIT, Jet Propulsion Lab., PR 20-204, Jan. 19, 1954.)

6. Dooley, D. A.: Combustion in Laminar Mixing Regions and Boundary Layers. Ph.D. Thesis in Aeronautics. CIT, Pasadena, Calif., 1956.

7. Morduchow, Morris: Analysis and Calculation by Integral Methods of Laminar Compressible Boundary Layer With Heat Transfer and With and Without Pressure Gradient. NACA Rep. 1245, 1955.

8. Jarre, Gianni: The Dissociation of a Pure Diatomic Gas in a Laminar Boundary Layer on an Adiabatic Flat Plate. Tech. Note 10. Laboratorio di Meccanica Applicata del Politecnico di Torino. Sept. 1958.

9. Penner, S. S.: Introduction to the Study of Chemical Reactions in Flow Systems. AGARDograph 7. Pergamon Press, N. Y., 1955. (Also published by Butterworth Sci. Pubs., London.)

10. Adamson, T. C., Jr., Nicholls, J. A., and Sherman, P. M.: A Study of the Hypersonic Laminar Boundary Layer With Dissociation. Part 1. Rep. 2606-6-T, Engineering Research Institute, Univ. of Mich., Ann Arbor, May 1957.

11. Hirschfelder, J. O.: Heat Transfer in Chemically Reacting Gas Mixtures. Jour. Chem. Phys., vol. 26, no. 2, Feb. 1957, pp. 274-281.

12. Huff, N. Vearl, Gordon, Sanford, and Morrelli, Virginia E.: General Method and Thermodynamic Tables for Computation of Equilibrium Composition and Temperature of Chemical Reactions. NACA Rep. 1037, 1951.

13. Keck, James: A Statistical Theory of Chemical Reaction Rates. AVCO Res. Rep. 20, Apr., 1958.

14. Heims, Steve P.: Effect of Oxygen Recombination on One-Dimensional Flow at High Mach Numbers. NACA TN 4144, 1958.

15. Camac, M., Camm, J., Feldman, S., Keck, J., and Petty, C.: Chemical and Radiative Relaxation in Air. AVCO Res. Lab. Semi-Annual Report on the Re-entry Problem, Section II, Part B, Dec. 1957, pp. II-50 - II-83.

16. Matthews, D. L.: Interferometric Measurement in the Shock Tube of the Dissociation Rate of Oxygen. The Physics of Fluids, vol. 2, no. 2, March-April 1959, pp. 170-178.

17. Scala, Sinclaire M., and Baulknight, Charles W.: Transport and Thermodynamic Properties in a Hypersonic Laminar Boundary Layer. Part 1. Properties of the Pure Species. ARS Journal, vol. 29, no. 1, Jan. 1959, pp. 39-45.

18. Feldman, Saul: Hypersonic Gas Dynamic Charts for Equilibrium Air. AVCO Res. Lab., Jan. 1957.

19. Schlichting, Hermann: Boundary Layer Theory. McGraw-Hill Book Co., Inc., 1955, p. 284.

20. Kuo, Y. H.: Dissociation Effects in Hypersonic Viscous Flows. Jour. Aero. Sci., vol. 24, no. 5, May 1957, pp. 345-350.

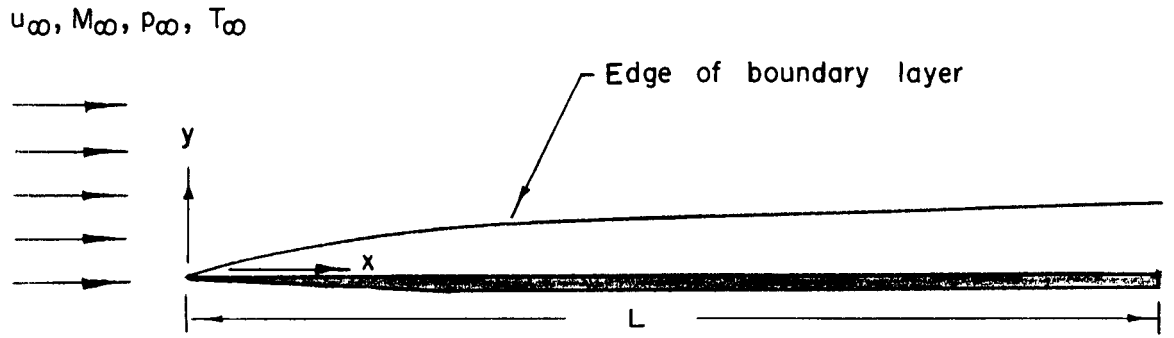

Figure 1.- Sketch of hypersonic laminar boundary layer over adiabatic flat plate.

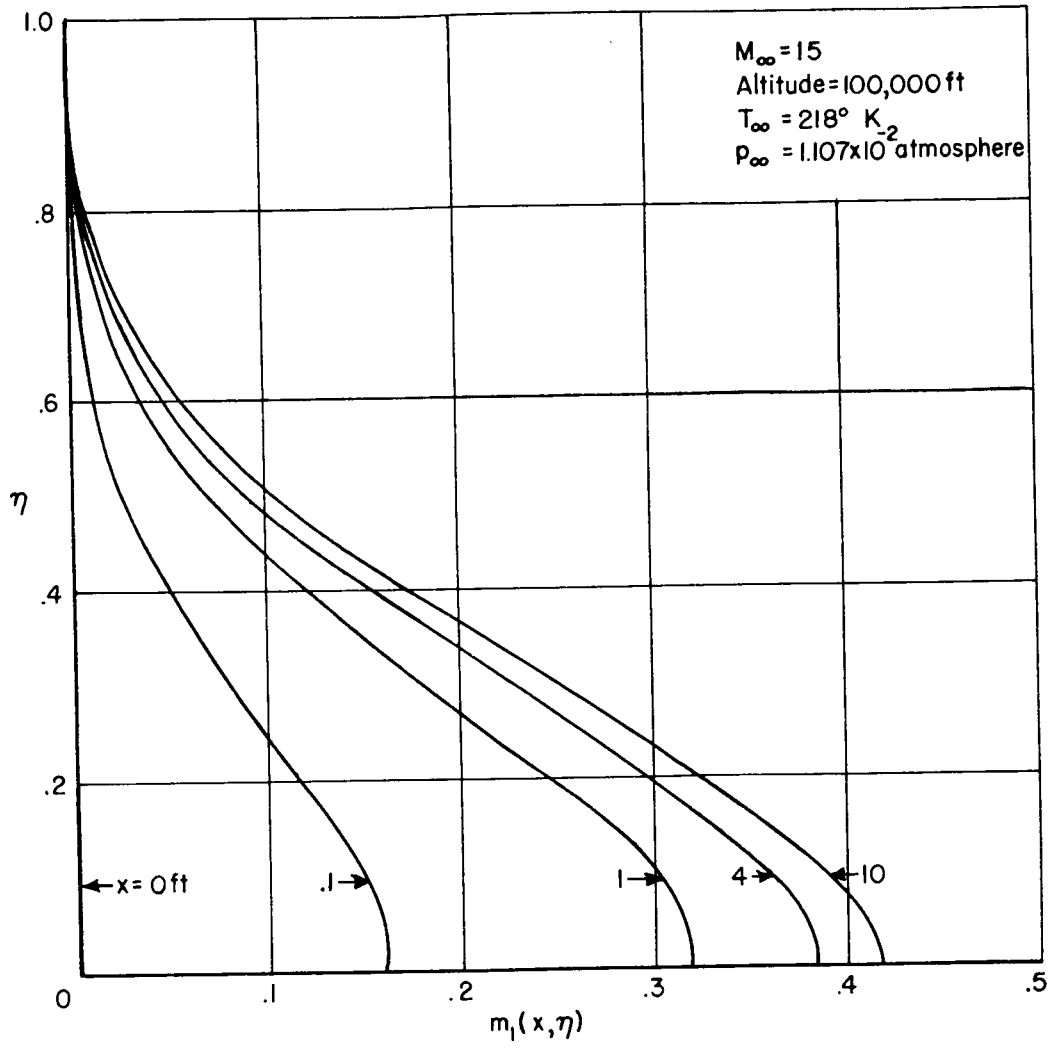

Figure 2.- Typical atom mass-fraction profile through boundary layer.

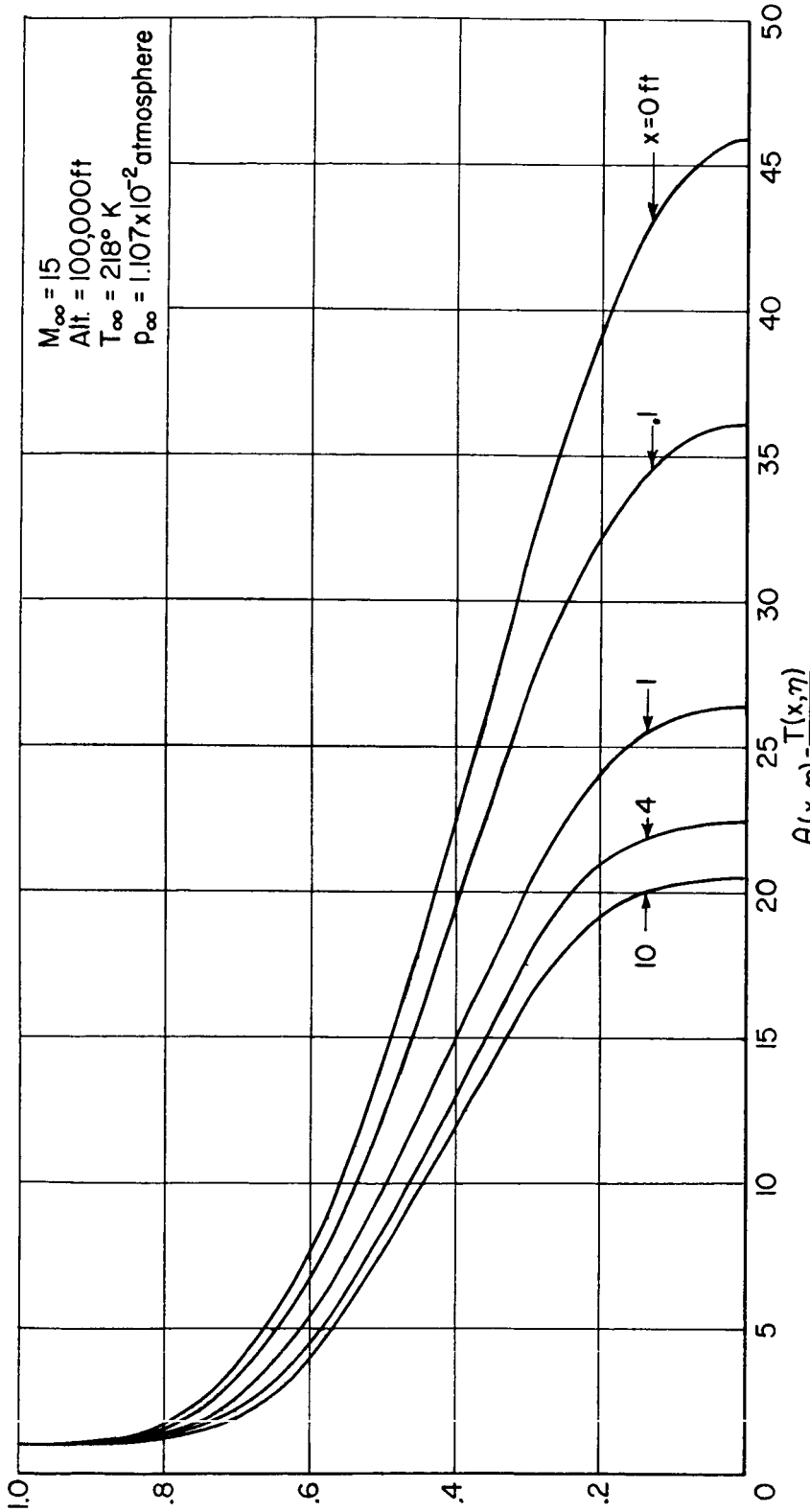

Figure 3.- Typical temperature profile through boundary layer.

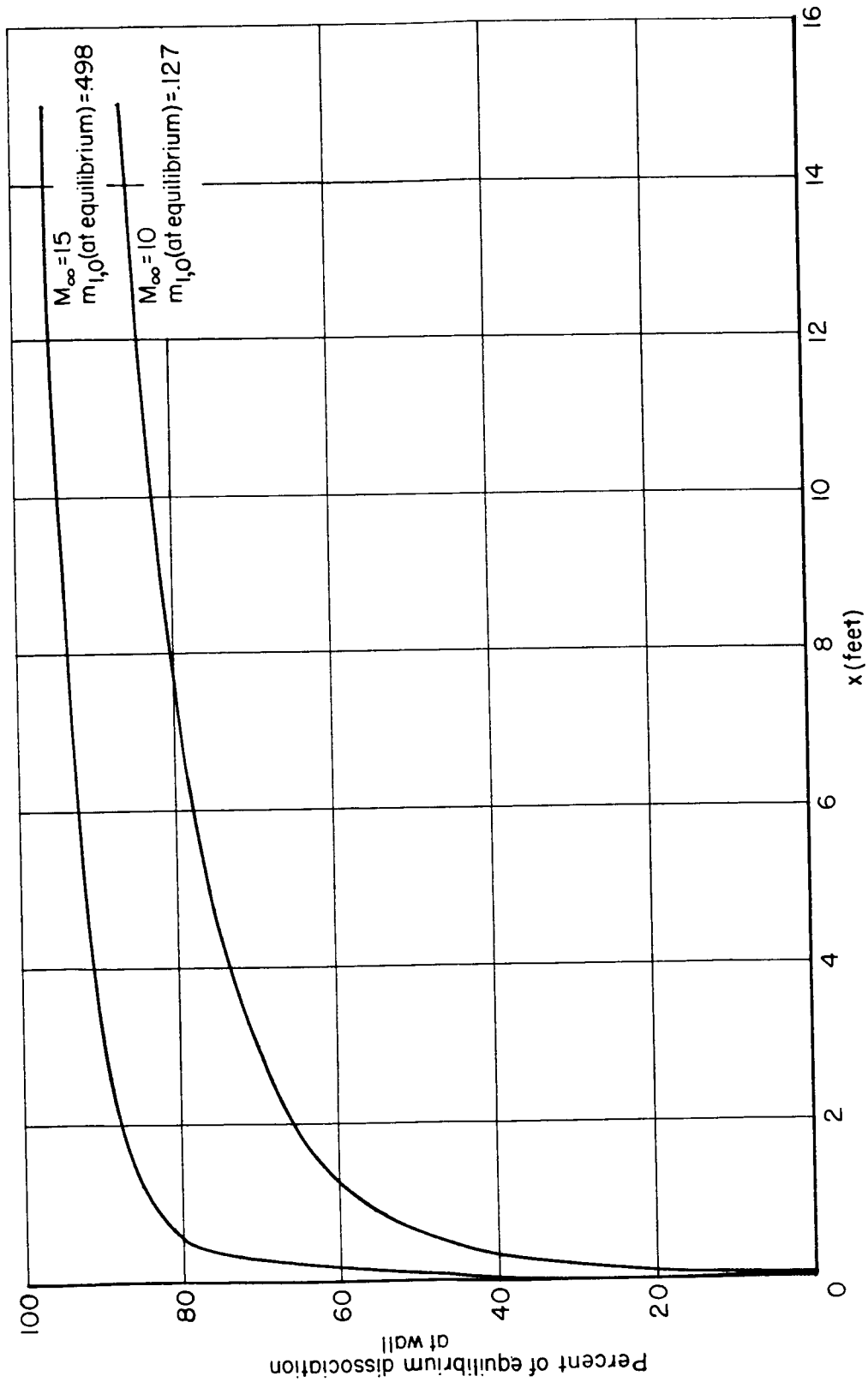

(a) Altitude = 50,000 feet; T_∞ = 218° K; p_∞ = 0.1161 atmosphere.

Figure 4.- Relaxation history at the wall.

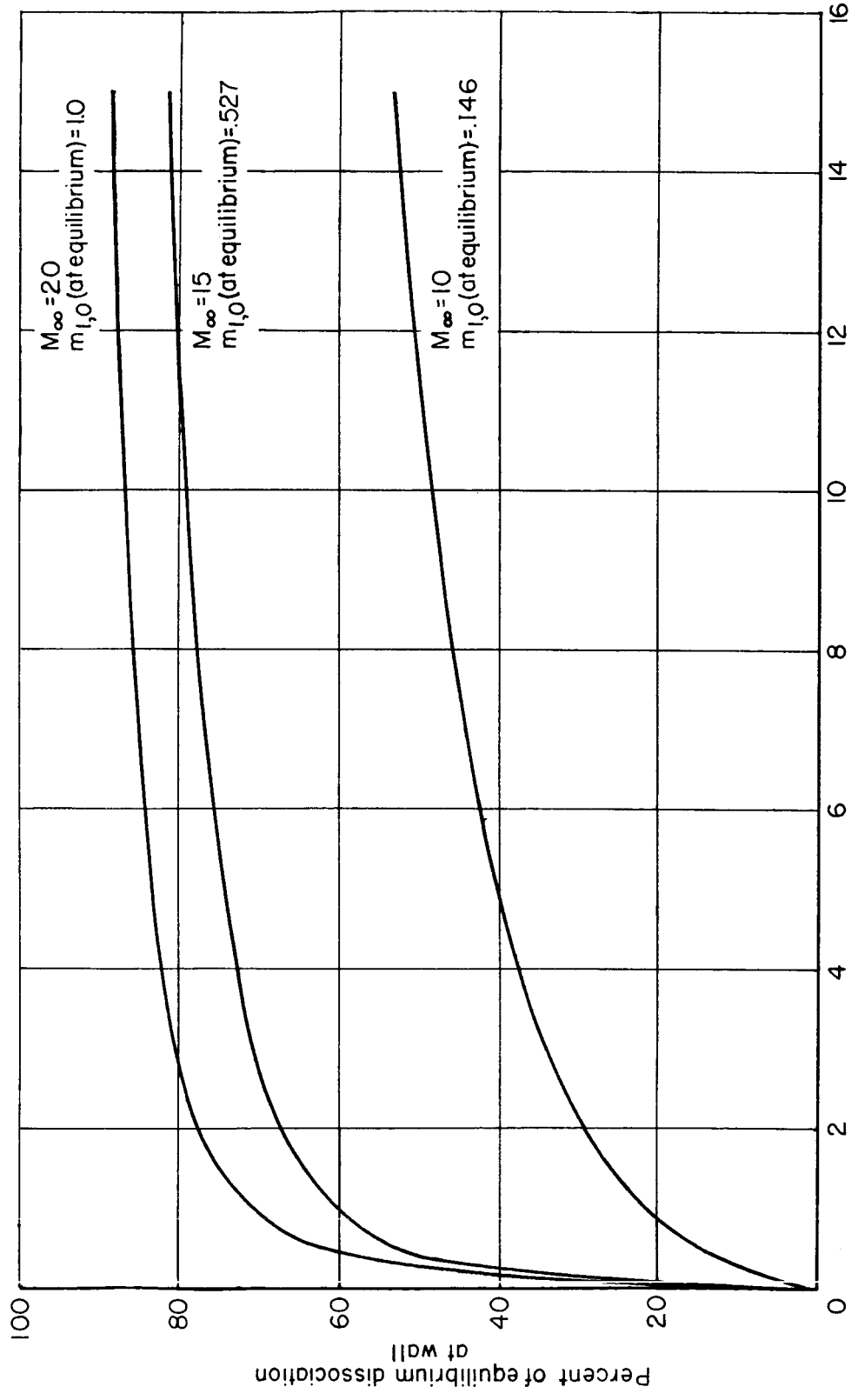

(b) Altitude = 100,000 feet; T_∞ = 218° K; p_∞ = 1.107×10^{-2} atmosphere.

Figure 4.- Continued.

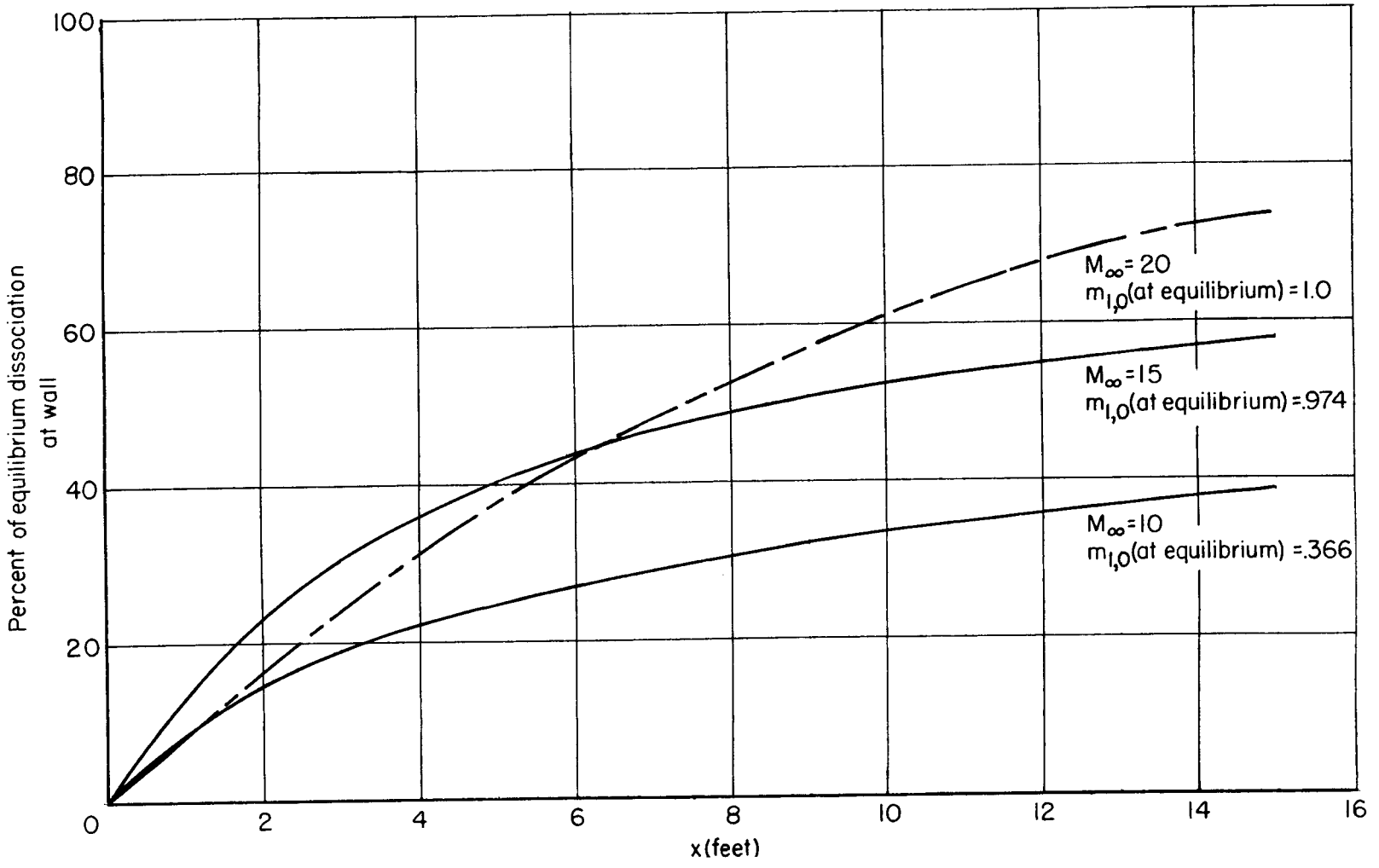

(c) Altitude = 200,000 feet; T_∞ = 348.9° K; p_∞ = 3.727×10^{-4} atmosphere.

Figure 4.- Concluded.

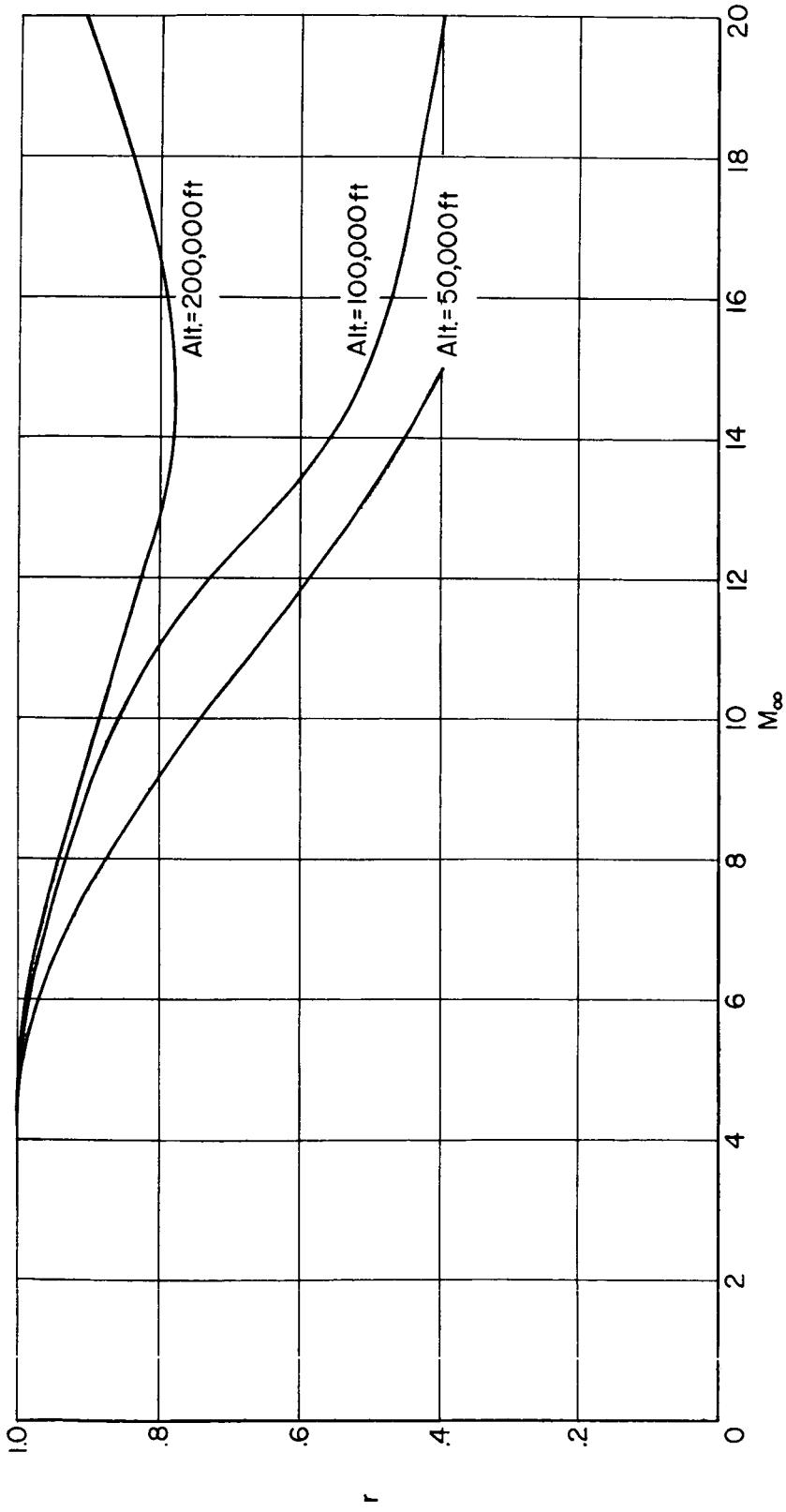

(a) x = 2.5 feet.

Figure 5.- Temperature recovery factor.

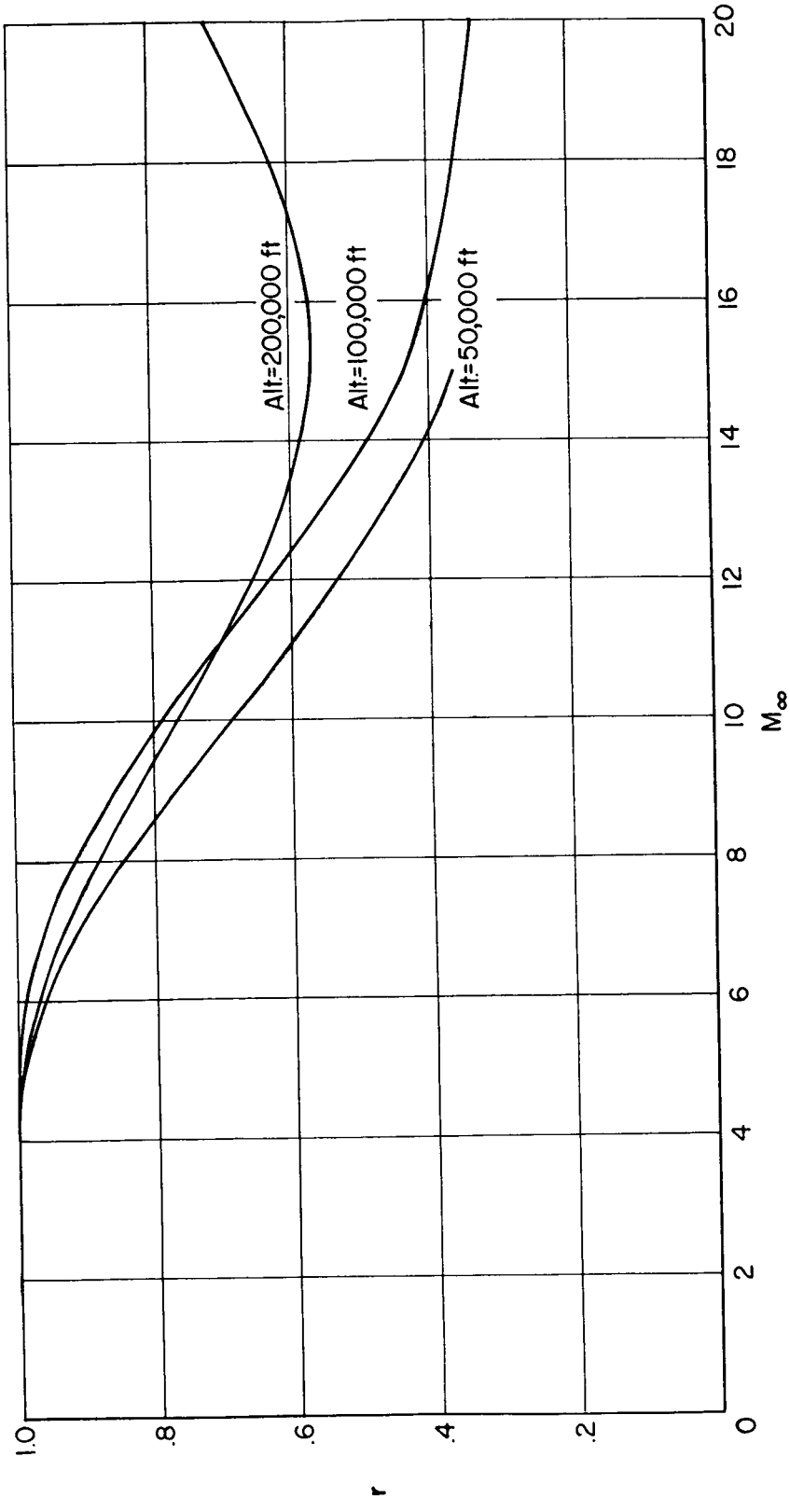

(b) x = 10 feet.

Figure 5.- Concluded.